Diving Deep onto Discriminative Ensemble of Histological Hashing & Class-Specific Manifold Learning for Multi-class Breast Carcinoma Taxonomy

Sawon Pratiher[§] and Subhankar Chattoraj[‡]
[§]*Department of Electrical Engineering, Indian Institute of Technology Kharagpur, WB, India*
[‡]*Department of Electronics & Communication Engineering, Techno India University, WB, India*

***Abstract*—Histopathological images (HI) encrypt resolution dependent heterogeneous textures & diverse color distribution variability, manifesting in micro-structural surface tissue convolutions & inherently high coherency of cancerous cells posing significant challenges to breast cancer (BC) multi-classification. As such, multi-class stratification is sparsely explored & prior work mainly focus on benign & malignant tissue characterization only, which forestalls further quantitative analysis of subordinate classes like adenosis, mucinous carcinoma & fibroadenoma etc, for diagnostic competence. In this work, a fully-automated, near-real-time & computationally inexpensive robust multi-classification deep framework from HI is presented.**

The proposed scheme employs deep neural network (DNN) aided discriminative ensemble of holistic class-specific manifold learning (CSML) for underlying HI sub-space embedding & HI hashing based local shallow signatures. The model achieves 95.8% accuracy pertinent to multi-classification, an 2.8% overall performance improvement & 38.2% enhancement for Lobular carcinoma (LC) sub-class recognition rate as compared to the existing state-of-the-art on well known *BreakHis* dataset is achieved. Also, 99.3% recognition rate at 200× & a sensitivity of 100% for binary grading at all magnification validates its suitability for clinical deployment in hand-held smart devices.

***Index Terms*—breast cancer; image hash; sub-space learning; discriminative ensemble; deep learning; deep neural networks.**

I. INTRODUCTION

Burgeoning cancer statistics in 2018 from World Cancer Report (WCR) estimate 2 million new cases of BC being registered worldwide [1]. World Health Organization (WHO) projects 627,000 women died from BC (which is approximately 15% of all cancer related deaths among women in 2018) & impacts 2.1 million women each year [2]. Significant research spanning imaging technique like computed tomography (CT), mammography, HI anatomization & magnetic resonance (MR) have been developed for early-stage BC prognosis through precision medicine initiative, but HI analysis is taken as the "gold standard" due to its rich encoded histological morphology & substantiating abnormal cellular activity. Additionally, deformation dynamics of these spatial tissue textures allows more specific characterizations from a diagnostic perspective [3] & aid pathologists to control growth & metastasis of tumor cells & devise therapeutic clinical schedules which are specific to particular sub-classes.

However, owing to ubiquitously abundant inhomogeneous morphology & complex intricate spatial correlations in the underlying inter-weaved biological tissue fabric of biopsy samples [4], automated machine vision for robust & accurate multi-class BC detection is still a challenging task & eludes researchers. Manual BC multi-classification by the pathologist is arduous & requires domain expertise with interpretations being subjective in nature. An automated computer-aided diagnostic (CAD) system overcome these challenges & assist clinicians in reliable diagnosis by reducing their workload & avoid erroneous diagnosis [5-6]. Further, practical CAD systems face challenges of inefficient hand-crafted feature engineering, which is computationally intensive & time consuming. Secondly, optimal supervised feature selection for accurate BC identification via image segmentation & identification of primitives like nuclei deformation, tubule formation, lymphocytes presence etc.,[7] & high-resolution HI analysis is computationally expensive requiring costly high-performance computation, which is generally not available in developing countries. Subtle inter-class & intra-class variability w.r.t., contrast & textures are evident in fig. 1. Fig. 1 shows representative Hematoxylin & Eosin (H&E) stained fine-grained multi-class biopsy tissue slides. (Taken from *BreaKHis* @400× magnification [8]). To resolve these challenges, a reliable &

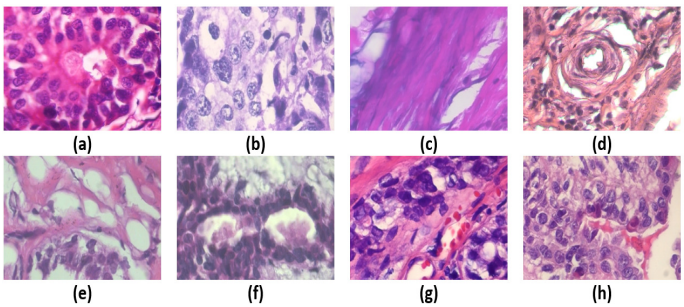

Figure 1: (a) Ductal carcinoma (DC), (b) Lobular carcinoma (LC), (c) Mucinous carcinoma (MC), (d) Papillary carcinoma (PC), (e) Adenosis, (f) Fibroadenoma, (g) Tubular adenoma (TA), (h) Phyllodes tumor (PT). (a) to (d) & (e) to (g) corresponds to malignant and benign class respectively.

more accurate practical method for BC multi-classification via DNN is developed. The proposed method discards feature engineering & employs end-to-end training of deep discriminative ensemble of holistic CSML of HI & local high-level to low-level semantic hierarchical hash signatures followed by softmax layer for classification. The model is validated with 7909 HI's to demonstrate its potency for deployment in clinical settings on generic processors & experimental result shows superior performance. The main contributions can be recapitulated as:

- A novel & scalable DNN for BC multi-classification framework is explored. The model, as shown in Fig. 2, yields the highest recognition rate with reduced computational time & complexity as compared to state-of-art.
- The scheme strengthen the intra-class morphological similarities & inter-class dissimilarities of the hierarchical feature space in a discriminative manner via deep ensemble of CSML & heterogeneous local hash signatures.

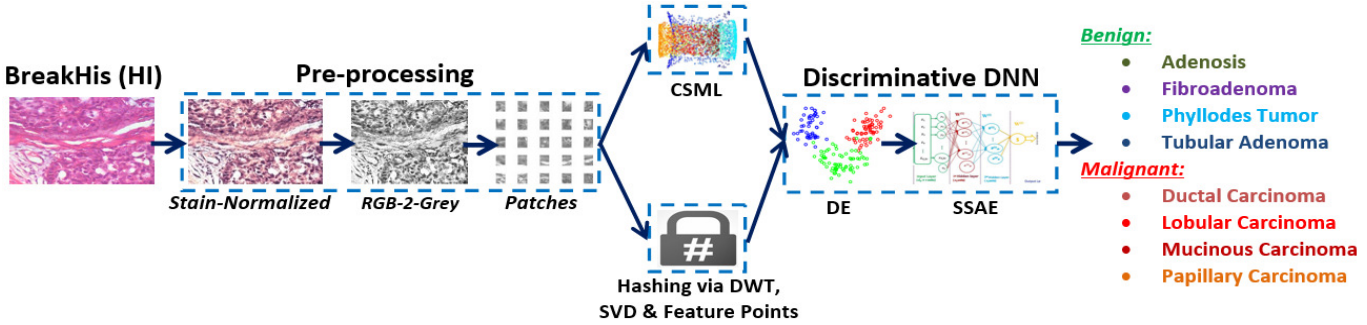

Figure 2: Stages of integrated pipeline: pre-processing, CSML & HI hash extraction, discriminative ensemble & DNN learning.

II. Materials & Prior Work

A. BreakHis Dataset

The proposed BC multi-classification method is examined on publicly available large-scale *BreaKHis* dataset [8] containing 7,909 H&E stained microscopic images from surgical biopsy (SOB) breast tumors, taken from 82 patients & collected at multiple magnification factor of: 40×,100×,200× & 400×. The images are of 700×460 pixels dimension with 24-bit color depth in 3-channel RGB (Red-Green-Blue) format. Table 1 summarizes the distribution of different histological sub-types & a detailed description can be traced from [8].

Table I: Distribution of classes, sub-classes in *BreaKHis* @ different magnification factors.

		Magnification Factor					
Class	**SC**	**40×**	**100×**	**200×**	**400×**	**Total**	**Patient**
M	DC	864	903	896	788	**3451**	58
	LC	156	170	163	137	**626**	
	MC	205	222	196	169	**792**	
	PC	145	142	135	138	**560**	
B	A	114	113	111	106	**444**	24
	F	253	260	264	237	**1014**	
	TA	109	121	108	115	**453**	
	PT	149	150	140	130	**569**	
Total		**1995**	**2081**	**2013**	**1820**	**7909**	**82**

B. Prior Art using BreaKHis

Significant research is concentrated around binary classification of benign & malignant classes. Over the past few years, researches have broadly investigated optimal feature engineering & deep learning based architectures. These can be found from the works of Spanhol et al., [8], ensemble classifier (EC) of shallow features by Gupta et al., [9], multiple feature vector (MFV) & transfer learning [10], graph-manifold & BI-LSTM models by Pratiher et al., [11], Grassmann manifold (GM) aided vector of locally aggregated descriptors (VLAD) by Dimitropoulos et al., [12] and convolution neural network (CNN) model with fusion rule (FR) [13]. Efficacy of ConvNet based fisher vector (CFV) & Gaussian mixture model (GMM) by Song et al., [14], deep CNN by Wei et al., [15] and BC classification using incremental boosting convolution networks in [16]. An exhaustive comparative study can be traced from Table III. Studies concerning multi-classification of sub-classes for clinical diagnosis or prognosis is done by Han Zhongyi et al., using class structured deep CNN (CSD-CNN) model [15] & Bardou et al. using CNN based approach [17]. Multi-classification BC histological research comparison can be found in Table IV & V.

III. Methodology & Related Theory

A. Experiment Design: *Deep Discriminative Ensemble of Histological Hashing & Class-Specific Manifold Learning*

Recently, DNN has shown efficacy in achieving state-of-the-art performance in diverse research problems spanning medical imaging [4], natural language processing (NLP) & speech processing. Here, we propose to use stacked sparse autoencoder (SSAE) based DNN [21] for robust BC multi-classification. Fig. 2 highlights the workflow. Our model pipeline consists of three main stages: Pre-processing stage for stain normalization, & overlapping & optimal patch segments of a specific size are generated for subsequent tissue index profile abstraction. Thereafter, class-specific manifold learning (CSML) of different histological sub-types are comprehended for nonlinear dimensionality reduction (NLDR). NLDR distillates discriminative low-dimensional structures pertinent to particular sub-class hidden in the high-dimensional HI. CSML preserves the intrinsic quasi-isometric geometry & local contour connectivity of HI point-cloud within tolerable limits via feature-space geometry constraints & is very much crucial for diagnosis. Thereafter, different hash signature obtained via discrete wavelet transform (DWT), singular-value decomposition (SVD) & perceptual feature-points augments the local shallow statistical HI descriptors. The holistic CSML & Hash vectors are fused in a discriminative fashion, which contemplates class structure based feature fusion. These ensemble discriminative super feature vectors are fed to SSAE for learning deep features & classification thereof.

B. Class-Specific Manifold Learning (CSML)

CSML is envisaged via Landmark Isomap (L-ISOMAP) aide Eigen sub-space estimation of a particular histological sub-type. For a vectorized HI point-cloud of Y data-points, arbitrarily $m(m \ll M)$ points are selected as Landmarks. Euclidean distance based embedding of the input data using m landmark points are selected from Y & followed by multi-dimensional scaling (MDS) using the $m \times m$ matrix $G_{m,M}$ of geodesic distances for each landmark pair to compute the low dimensional feature space. Mathematically, it is given by:

$$m^T(p,q) = -\frac{1}{2}\left(F_{pq}^2 - e_p \frac{1}{m}\sum_l H_{pl}^2\right), \qquad (1)$$

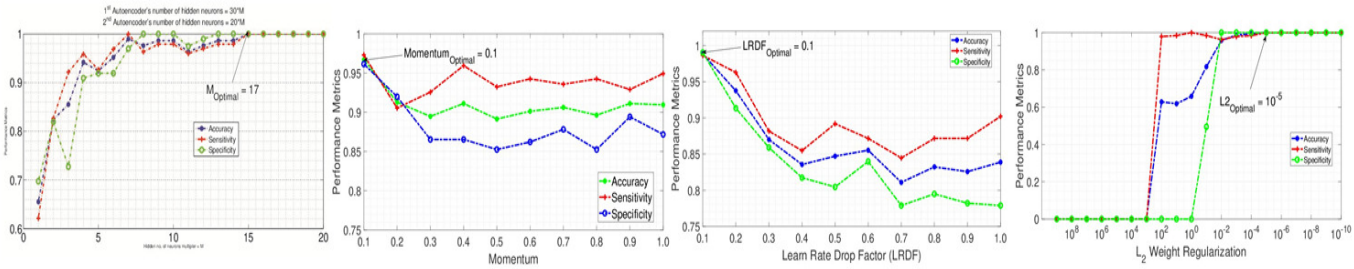

Figure 3: Hyper-parameter tuning in DNN. (a) hidden size, (b) momentum, (c) learn rate drop factor, (d) L_2 weight regularization

where, H^2 is the means geodesic distance matrix H is element-wise squared & e_p is the Eigen vector with zero Eigen value. Details about L-ISOMAP can be traced from [22].

C. Histological Hashing for Local Signatures

Rudimentary image hashing details can be found in [23-26]. Histological image hashing encodes locality reference & inherent neighborhood connectivity of the underlying HI. Here, we have used the following hash signatures:

1) Discrete Wavelet Transform (DWT) Based Image Hash: Computes robust & compact hash via 2D DWT on HI, which decomposes into four sub-bands. Both edge or high frequency information & coarse stable low-frequent coefficients are perceived via DWT coefficients [23].

2) Hashing Via Singular Value Decomposition (SVD): SVD based image hasing has robust tolerance to small rotational changes until 10 & is translation in-variance & incorporates low rank approximation of original normalized sub-image of HI & non-correlated directional feature space encoding [24].

3) Feature Point Based Image Hashing: Statistical image features like Hessian affine, maximally stable extremal region (MSER) detectors, Harris corner detector & feature points based on end-stopping behavior like end-stopped Wavelets such as Morlets preserves the momentous image geometry feature-space constraints of 2-D HI pixels & mapped to 1-D feature vector which is compressed to generate the hash vector [25].

D. SSAE aided DNN Training & Hyper-parameters Tuning

Discriminative feature ensemble of holistic CSML & shallow hash signatures is fused via discrimination correlation analysis [27]. Stacked Sparse Autoencoder (SSAE) [28] involves optimal parameter $\theta = (V, a_k, a_y)$ computation by minimizing the error between the model input and output. Rudimentary details can be traced from [21]. The model is trained on a generic system woth mode configuration as 3.50 GHz processor, 16GB RAM & AMD FX-8320 Octa-core. Fig 3 shows hyper-tuned optimal SSAE parameters. A maximum epoch of 500 & number hidden layer neurons in the first and second autoencoders (AE) is kept at 500 & 300 respectively. Further, L_2 weight regularization, sparsity regularization & sparsity proportion in the two AE are set to 0.001, 4 & 0.15. '*tanh*' activation function (AF) in the hidden units is connected to by fully connected layer & classification done via a softmax layer. '*tanh*' AF is used due to its robust tolerance to approximate intrinsic manifold non-linearity & extraction of mutual dependence for further segregation thereof. Piece-wise back propagation learning via stochastic gradient descent (SGD) algorithm is envisaged with a learning rate of 10^{-4} & the initial random weights drawn uniformly from $[-0:1; 0:1]$, gradient decay factor of 0.2, momentum of 0.6, learning rate drop period (LRDP) of 5 & L_2 weight regularization of 10^{-4} is used during the training phase. The weights (W) & bias (b) are updated as

$$W_l = W_l - \eta \frac{\partial}{\vartheta W_l}(W, b; X, t) = B_l W_l - \eta \frac{\partial}{\vartheta B_l}(W, B; X, t) \quad (2)$$

where, W_l represents the weights, B_l represents the l^{th} layer bias, η is learning rate, (X,t) is the mini-batch comprising of *'m'* training samples. In order to eschew skewed model over-fitting & bias minimization, the data is randomly partitioned in the ratio 60:20:20 for to training, validation & testing phase.

IV. Results and Discussion

The adequacy of the proposed method is evaluated in terms of standard evaluation metrics i.e., classification accuracy (AC), sensitivity (SN) & specificity (SP). Experimental results for both binary & multi-classification are compared with state-of-the-art techniques on benchmark *BreaKHis* dataset.

Table II: Results for Binary Classification. PM = Performance Metrics

Class	PM (%)	Magnification Factor			
		40X	**100X**	**200X**	**400X**
Binary	AC	99.1	98.7	**99.3**	98.4
	SN	**100**	**100**	**100**	**100**
	SP	98.3	97.9	**98.5**	96.8

A. Grading Tumor Malignancy: Binary Classification

Initially, binary classification of BC into benign & malignant classes is done to ensure its competence in coarse HI characterization. Table II highlights the performance measure of the experimental results for different magnification factors. 100% sensitivity for all magnification factor ensures that all malignant classes are recognized correctly. As such, pathologist may invest more time for identifying benign cases with our system & demonstrates the effectiveness of the DNN model to learn deep malignancy biomarkers for discriminative HI grading. A comparative study of the proposed mode with the existing state-of-the-art methods [8-20] is given in Table III. It may be noted that the proposed framework outperforms all the previously used methods in terms of classification accuracy with a significant enhancement at all magnification factors. Further, our proposed discriminative DNN framework

outperforms the conventional & visual feature descriptor based approach such LBP [8], VLAD [12] and KAZE [20] & also surpasses recent CNN & BiLSTM based methods [10-11][14-16], which is proved to be optimal in analyzing visual imagery. This indicates that our proposed system which is robust in terms of performance & computationally much more efficient as it runs on generic laptops as compared to CNN models which requires graphics processing unit (GPU).

Table III: State-of-the-art comparison for binary classification of benign and malignant classes

Ref, Years	Feature + Method	Performance (%)			
		40X	100X	200X	400X
[13], 2016	CNN, FR	85.6	83.5	82.7	80.7
[8] 2016,	CLBP, SVM	77.40	76.40	70.20	72.80
[9], 2017	C-TID, EC	87.2	88.22	88.89	85.82
[10], 2017	CNN, DeCAF, MFV	84.6	84.8	84.2	81.6
[11], 2017	GML, BI-LSTM	96.2	97.2	97.1	95.4
[12], 2017	VLAD, GM	91.8	92.1	91.4	90.2
[14], 2017	I-EM, CFV, CNN, GMM	87.7	87.6	86.5	83.9
[15], 2017	CSDCNN	95.8	96.9	96.7	94.9
[16], 2018	DCNN	95.1	96.3	96.9	93.8
[17], 2018	Dense SIFT, SURF, BOW, LCLC	98.33	97.12	97.85	96.15
[18], 2018	FV, CSE	87.5	88.6	85.5	85.0
[19], 2018	TL, DenseNet	84.72	89.44	95.65	82.65
	CNN, DenseNet	91.90	93.64	95.84	90.15
	MV, XGboost	94.71	95.9	96.76	89.11
[20]	KAZE, BOF, binary SVM	85.9	80.4	78.1	71.1
This Work	**CSML, Hashing DNN**	**99.1**	**98.7**	**99.3**	**98.4**

B. Multi-classification Performance

It's evident from literature survey that there are very few literature available in the multi-class classification of BC from HI & as such, we further examine the proposed framework towards the multi-class classification of BC to demonstrate its efficacy towards practical use from a clinical perspective. State-of-the-art comparative evaluation is given in Table IV, whereas Table V gives class specific performance accuracy. It is evident that the proposed discriminative DNN framework not only surpasses the state-of-art on the basis of magnification factor but also on the basis of HI sub-classes in terms of recognition rate. Earlier in the state-of-art, CSDCNN [15] based approach exhibited best recognition rate for multi-class classification but our proposed method surpasses it in all the magnification factor by **3.3%, 1.8%, 2.6%, 3.5%**, for $40\times$, $100\times$, $200\times$ & $400\times$ magnification. Table V shows that our method surpasses the class-specific recognition rate with high margin & in some case as high as **38.2%** enhancement for Lobular carcinoma (LC) sub-class.

Table IV: State-of-the-art comparison for multi-Classification histological sub-types

Ref	Feature + Method	Performance (%)			
		40X	100X	200X	400X
[15]	CSDCNN	92.8	93.9	93.7	92.9
[17]	DSIFT + BoW	41.80	38.56	49.75	38.67
	SURF + BoW	53.07	60.80	70.00	51.01
	DSIFT + LLC	60.58	57.44	70.00	49.96
	SURF + LLC	80.37	63.84	74.54	54.70‘
	DSIFT, BoW +SVM	18.77	17.28	20.16	17.49
	SURF, BoW+ SVM	49.65	47.00	38.84	29.50
	DSIFT, LLC+SVM	48.46	49.44	43.97	32.60
	SURF, LLC+ SVM	55.80	54.24	40.83	37.20
	CNN, SVM-RBF	75.43	71.20	67.27	65.12
This Work	**CSML, Hashing, DNN**	**95.1**	**95.7**	**95.8**	**95.2**

Table V: Class-specific performance comparison with [17]

Class	Ref, years	SC	Magnification Factor			
			40×	100×	200×	400×
Malignant	[17], 2018	DC	91.51	90.77	91.14	92.74
	This Work	DC	**96.7**	**97**	**97.6**	**96.9**
	[17], 2018	LC	78.72	54.90	63.27	56.10
	This Work	LC	**93.8**	**94.7**	**92.8**	**93.1**
	[17], 2018	MC	70.49	82.09	61.02	70.59
	This Work	MC	**94.4**	**95.8**	**96.6**	**94.9**
	[17], 2018	PC	67.44	83.72	57.50	68.29
	This Work	PC	**93.1**	**95.2**	**93**	**93.1**
Benign	[17], 2018	A	85.29	79.41	84.85	90.63
	This Work	A	**93.5**	**93.9**	**97**	**94.1**
	[17], 2018	F	86.84	91.03	91.14	77.46
	This Work	F	**95**	**95.6**	**94.9**	**95.1**
	[17], 2018	TA	75.56	93.33	76.19	82.05
	This Work	TA	**94.5**	**94.1**	**94.3**	**94.4**
	[17], 2018	PT	76.19	63.89	62.50	58.82
	This Work	PT	**94.4**	**95.1**	**95.2**	**94.7**

V. CONCLUSION

A novel deep discriminative ensemble learning CAD for multi-class BC characterization is introduced in this work. The method implements deep contextual grading of hybrid holistic-level CSML representations & local hash signatures of HI, thereby, effectively discriminating between benign & malignant sub-classes. The proposed approach was validated using *BreakHis* dataset & experimental results exemplify superior discriminating performance as compared to the existing state-of-the-art. In particular, it shows high specificity towards malignant sub-classes, which can assist pathologists by reducing their heavy workload & arrange optimal therapeutic schedules for further diagnosis or prognosis of benign tissues.

Currently, the method is being escalated to include deeper structures using graph CNN & sequential contextual learning with other tissue images to investigate the diagnostic modality.

REFERENCES

[1] https://www.wcrf.org/dietandcancer/cancer-trends/breast-cancer-statistics

[2] https://www.who.int/cancer/prevention/diagnosis-screening/breast-cancer/en/

[3] Stenkvist, Bjrn, et al. "Computerized nuclear morphometry as an objective method for characterizing human cancer cell populations". Cancer research 38.12 (1978): 4688-4697.

[4] Boucheron, Laura E., B. S. Manjunath, and Neal R. Harvey. "Use of imperfectly segmented nuclei in the classification of histopathology images of breast cancer." Acoustics Speech and Signal Processing (ICASSP), 2010 IEEE International Conference on. IEEE, 2010.

[5] Kowal, Marek, et al. "Computer-aided diagnosis of breast cancer based on fine needle biopsy microscopic images". Computers in biology and medicine 43.10 (2013): 1563-1572.

[6] Lacquet, F. A., et al. "Slide preparation and staining procedures for reliable results using computerized morphology." Archives of andrology 36.2 (1996): 133-138

[7] M. N. Gurcan, L. E. Boucheron, A. Can, A. Madabhushi, N. M. Rajpoot and B. Yener, "Histopathological Image Analysis: A Review," in IEEE Reviews in Biomedical Engineering, vol. 2, pp. 147-171, 2009. doi: 10.1109/RBME.2009.2034865

[8] Spanhol, Fabio A., et al. "A dataset for breast cancer histopathological image classification." IEEE Transactions on Biomedical Engineering 63.7 (2016): 1455-1462.

[9] Gupta, Vibha, and Arnav Bhavsar. "Breast Cancer Histopathological Image Classification: Is Magnification Important?." Proceedings of the IEEE Conference on Computer Vision and Pattern Recognition Workshops. 2017.

[10] Fabio A. Spanhol, Paulo R. Cavalin y, Luiz S. Oliveira, Caroline Petitjean, and Laurent Heutte, "Deep Features for Breast Cancer Histopathological Image Classification",2017 IEEE International Conference on Systems, Man, and Cybernetics (SMC).

[11] S. Pratiher, S. Chattoraj, S. Agarwal and S. Bhattacharya, "Grading Tumor Malignancy via Deep Bidirectional LSTM on Graph Manifold Encoded Histopathological Image," 2018 IEEE International Conference on Data Mining Workshops (ICDMW), Singapore, Singapore, 2018, pp. 674-681. doi: 10.1109/ICDMW.2018.00104

[12] Dimitropoulos K, Barmpoutis P, Zioga C, Kamas A, Patsiaoura K, Grammalidis N (2017), "Grading of invasive breast carcinoma through Grassmannian VLAD encoding". PLoS ONE 12(9): e0185110. https://doi.org/10.1371/journal.pone.0185110

[13] F. A. Spanhol, L. S. Oliveira, C. Petitjean and L. Heutte, "Breast cancer histopathological image classification using Convolutional Neural Networks," 2016 International Joint Conference on Neural Networks (IJCNN), Vancouver, BC, 2016, pp. 2560-2567. doi: 10.1109/IJCNN.2016.7727519

[14] Song Y., Chang H., Huang H., Cai W. (2017) "Supervised Intra-embedding of Fisher Vectors for Histopathology Image Classification", Medical Image Computing and Computer-Assisted Intervention - MICCAI 2017 Lecture Notes in Computer Science, vol 10435. Springer, Cham

[15] B. Wei, K. Li, S. Li, Y. Yin, Y. Zheng, Z. Han, "Breast cancer multi-classification from histopathological images with structured deep learning model Sci Rep, 7 (2017), p. 4172, https://doi.org/10.1038/s41598-017-04075-z.

[16] Vo, Duc My, Ngoc-Quang Nguyen, and Sang-Woong Lee."Classification of breast cancer histology images using incremental boosting convolution networks." Information Sciences 482 (2019): 123-138.

[17] D. Bardou, K. Zhang and S. M. Ahmad, "Classification of Breast Cancer Based on Histology Images Using Convolutional Neural Networks," in IEEE Access, vol. 6, pp. 24680-24693, 2018. doi: 10.1109/ACCESS.2018.2831280

[18] Yang Song, Hang Chang, Yang Gao, Sidong Liu, Donghao Zhang, Junen Yao, Wojciech Chrzanowski & Weidong Cai, "Feature learning with component selective encoding for histopathology image classification" 2018 IEEE 15th International Symposium on Biomedical Imaging (ISBI 2018).

[19] Vibha Gupta, Arnav Bhavsar "Sequential Modeling of Deep Features for Breast Cancer Histopathological Image Classification", The IEEE Conference on Computer Vision and Pattern Recognition (CVPR) Workshops, 2018, pp. 2254-2261.

[20] Sanchez-Morillo D., González J., García-Rojo M., Ortega J. (2018) Classification of Breast Cancer Histopathological Images Using KAZE Features. In: Rojas I., Ortuño F. (eds) Bioinformatics and Biomedical Engineering. IWBBIO 2018. Lecture Notes in Computer Science, vol 10814. Springer, Cham.

[21] Bose, Tulika, Angshul Majumdar, and Tanushyam Chattopadhyay. "Machine Load Estimation Via Stacked Autoencoder Regression." 2018 IEEE International Conference on Acoustics, Speech and Signal Processing (ICASSP). IEEE, 2018.

[22] H. Shi, B. Yin, X. Zhang, Y. Kang and Y. Lei, "A landmark selection method for L-Isomap based on greedy algorithm and its application," 2015 54th IEEE Conference on Decision and Control (CDC), Osaka, 2015, pp. 7371-7376. doi: 10.1109/CDC.2015.7403383

[23] Tang, Zhenjun, et al. "Robust image hashing via colour vector angles and discrete wavelet transform." IET Image Processing 8.3 (2013): 142-149.

[24] Kozat, Suleyman Serdar, Ramarathnam Venkatesan, and Mehmet Kivanç Mihçak. "Robust perceptual image hashing via matrix invariants." 2004 International Conference on Image Processing, 2004. ICIP'04. Vol. 5. IEEE, 2004.

[25] Monga, Vishal, and Brian L. Evans. "Perceptual image hashing via feature points: performance evaluation and tradeoffs." IEEE transactions on Image Processing 15.11 (2006): 3452-3465.

[26] Li, Yuenan, and Ping Wang. "Robust image hashing based on low-rank and sparse decomposition." Acoustics, Speech and Signal Processing (ICASSP), 2016 IEEE International Conference on. IEEE, 2016.

[27] Haghighat, Mohammad, Mohamed Abdel-Mottaleb, and Wadee Alhalabi. "Discriminant correlation analysis for feature level fusion with application to multimodal biometrics." Acoustics, Speech and Signal Processing (ICASSP), 2016 IEEE International Conference on. IEEE, 2016.

[28] Qi, Yu, et al. "Robust feature learning by stacked autoencoder with maximum correntropy criterion." Acoustics, Speech and Signal Processing (ICASSP), 2014 IEEE International Conference on. IEEE, 2014.